https://doi.org/10.15407/scine18.06.097

PYLYPENKO, O. V. (http://orcid.org/0000-0002-7583-4072),
DOLGOPOLOV, S. I. (http://orcid.org/0000-0002-0591-4106),
NIKOLAYEV, O. D. (http://orcid.org/0000-0003-0163-0891),
KHORIAK, N. V. (http://orcid.org/0000-0002-4622-2376),
KVASHA, Yu. A. (http://orcid.org/0000-0002-5910-0407),
and BASHLIY, I. D. (http://orcid.org/0000-0003-0594-9461)
Institute of Technical Mechanics of the National Academy of Sciences
of Ukraine and State Space Agency of Ukraine,
15, Leshko-Popelya St., Dnipro, 49005, Ukraine,
+380 56 372 0640, +380 56 372 0640, office.itm@nas.gov.ua

DETERMINATION OF THE THRUST SPREAD IN THE *CYCLONE-4M* FIRST STAGE MULTI-ENGINE PROPULSION SYSTEM DURING ITS START

Introduction. *The development of the Cyclone-4M space rocket complex is an important project of Ukraine space industry. In order to reduce the costs and the time inputs for the design and manufacture of liquid rocket engines (LRE) for the 1st stage of the Cyclone-4M launch vehicle, Pivdenne Design Office has employed the clustered multi-engine prototyped before as 1st stage sustainer engine.*

Problem Statement. *In a clustered multi-engine propulsion system, because of internal and external factors, individual engines do not start simultaneously. This may lead to dangerous spreads in the thrust of individual LREs in the course of the start of propulsion system, which can cause significant deviations of the launch vehicle motion from its trajectory within the initial time interval of the flight.*

Purpose. *The purpose of this research is to estimate the thrust spread as a result of the effect of internal and external factors on the transient processes in the individual engine systems and their dynamic interaction during the start of a multi-engine system of the Cyclone-4M first stage.*

Material and Methods. *The methods of automatic control theory, the impedance method, the statistical method and the methods for numerical simulation of non-stationary processes in pipeline systems of launch vehicles have been used.*

Results. *A mathematical model for start of multi-engine propulsion system of the Cyclone-4M first stage has been developed. It makes it possible to take into account the influence of spread of internal and external factors on the transient processes in a multi-engine system during the start of the engines. An effective method for determining the indicated thrust spread, which is based on the use of LP_τ-sequences (Sobol sequences) that are sequences of multidimensional points whose uniform distribution is asymptotically optimal, has been developed. The transient processes in the RD-874 multi-engine propulsion system have been determined for various combinations of engine misalignments caused by external and internal factors. The lower and upper envelope curves of the time dependences of combustion chamber pressure have been plotted for each LRE in the multi-engine propulsion system.*

Conclusions. *The thrust spread and the spread of the time of reaching 90% thrust for RD-874 multi-engine propulsion system is significantly (about 2 times) smaller than that for individual RD-870 engine in this propulsion system.*

Keywords: liquid-propellant rocket engine, multi-engine liquid-propellant rocket launch vehicle, start, mathematical modeling, external and internal factors, and thrust spread.

Citation: Pylypenko, O. V., Dolgopolov, S. I., Nikolayev, O. D., Khoriak, N. V., Kvasha, Yu. A., Bashliy, I. D. Determination of the Thrust Spread in the *Cyclone-4M* First Stage Multi-Engine Propulsion System During its Start. *Sci. innov.*, 18(6), 97—112. https://doi.org/10.15407/scine18.06.097

Currently, one of the important projects of the space industry of Ukraine is the development of the *Cyclone-4M* space rocket complex [1] at *Pivdenne* Design Office, with the involvement of other enterprises of the space industry and the National Academy of Sciences of Ukraine. In order to reduce the costs and time inputs for designing and manufacturing liquid rocket engines for the first stage of *Cyclone-4M* launch vehicle, *Pivdenne* Design Office has been going to employ the four-engine cluster that was prototyped before [2] as 1st stage sustainer engine. The use of such an approach opens up the prospects for a quick and reliable creation of LRE for the *Cyclone-4M* first stage by including the necessary number of engines in the cluster.

All LREs have a thrust spread and different time of 90% thrust takeoff because of the internal (temperature in gas tracts, turbine and pump efficiency, pump head, etc.) and the external (pressure and temperature of fuel components at the engine inlet) factors. In multi-engine device, the interaction of individual LRE and the combination of the internal and external factors of individual engines may lead to dangerous thrust spreads in both individual LREs as part of the rocket engine and the rocket engine as a whole during its start. Such an extraordinary situation, at best, may lead to a significant deviation of the launch vehicle motion from the base trajectory at the initial stage of its flight, and in the worst case, may result in a start failure. The mathematical modeling of the low-frequency dynamics of the *Cyclone-4M* multi-engine and the study of the effect of internal and external factors on the dynamic processes during the start of individual LREs in the cluster and the rocket engine as a whole allow predicting and preventing possible emergency situations during the start of *Cyclone-4M* launch vehicle.

The purpose of this research is to estimate the thrust spread as a result of the effect of internal and external factors on the transient processes in the individual engine systems and their dynamic interaction during the start of a multi-engine system of the *Cyclone-4M* first stage.

MATHEMATICAL MODEL OF THE START OF CYCLONE-4M FIRST STAGE MULTI-ENGINE

The *Cyclone-4M* first stage multi-engine RD-874 includes four RD-870 engines. Figure 1 *a, b* shows a layout of the feed lines of shared propulsion system and simplified flow schematic of this engine (main oxidizer pipe in Fig. 1 *a* and RD-870 engine in Fig. 1 *b*; each RD-870 engine is supplied with fuel from a tank fuel through a separate pipeline). The RD-870 engines are made according to the scheme using generator gas afterburning process and have a higher specific thrust impulse as compared with the engines without afterburners. Thanks to this, the former have prospects for their wide use in the future.

The mathematical model of the RD-874 start describes all significant low-frequency dynamic processes in the sustainer engine and takes into account a large number of internal factors associated with dynamic processes in engines. Such models differ in their complex structure and include dozens and even hundreds of differential and algebraic equations [3]. Below, we briefly consider individual fragments of the complete mathematical model of the RD-874 start, which describe the most significant low-frequency dynamic processes in the sustainer engine.

Such a model should include equations describing the process of filling hydraulic tracts with fuel components. The process of filling the hydraulic tracts occurs at the initial stage of the LRE start and significantly affects the ignition time of the fuel components in the gas generator and, in general, the characteristics of the LRE start. In order to describe the dynamics of the liquid in the hydraulic tracts of the LRE, the section of the tract to be filled is divided into several sections with similar volumes. The equation for filling the i-th section is written as

$$\frac{dV_{Li}}{dt} = \frac{G_{Li} - G_{EKi} - G_{PXi}}{\gamma_{Li}},$$

where V_{Li}, γ_{Li} are the volume of i-th section to be filled and the specific gravity of the liquid in the

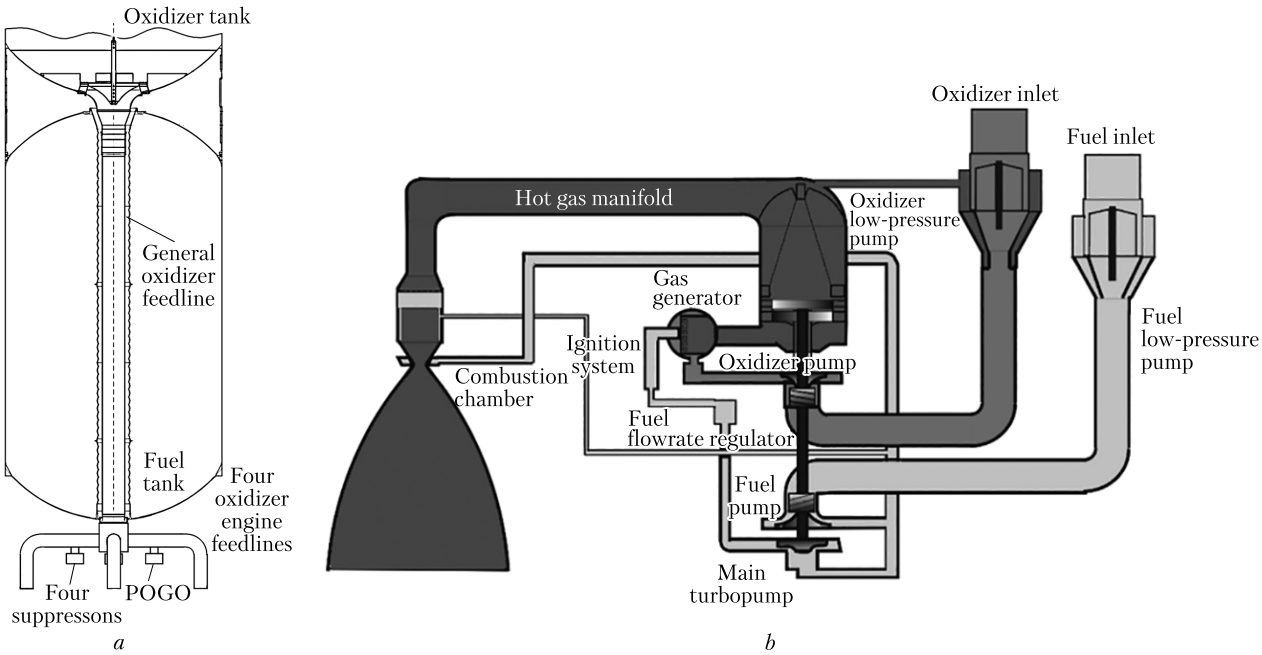

Fig. 1. Simplified flowchart of the oxidizer trunk of RD-874 multi-engine propulsion system (*a*) and RD-870 LRE (*b*)

section, respectively; t is time; G_{Li} is consumption of the liquid phase to fill the i-th section; G_{EKi} is the sum of liquid consumption (greater than zero, liquid boiling) and steam consumption (less than zero, steam condensation) when the parameters (pressure and temperature) of liquid and steam pass through the saturation curve; G_{PXi} is the flow rate of a liquid that converts into steam when heated. The shape of the filling front, which is determined by the experimental filling function, has a decisive influence on the filling characteristics of hydraulic tracts. In the case of cryogenic fuel components, determining the filling of hydraulic tracts is significantly complicated [4]. It is necessary to additionally take into account the heating of the cryogenic propellant, its gasification and condensation, as well as the cooling of the structure of the hydraulic tract.

In the RD-870 engines, a gas turbine is used as a drive for the oxidizer booster pump, the working fluid of which is the gas taken after the main turbine. According to the engine scheme, the exhaust gas is discharged into the flow of the liquid (cryogenic) component of the fuel at the inlet of the main oxidizer pump. The condensing gas carries a potential danger of the instability of the work process because of both the destabilization of the gaseous working fluid condensation during the transient processes and the possible cavitation self-oscillations in the hydraulic system that consists of a short pipeline and the main oxidizer pump. To take into account the injection of a gaseous working medium into the fuel liquid component flow, for the mathematical modeling of the start of the RD-870 rocket engine, the authors have used the generalized results of experimental studies of the condensation of superheated oxygen vapor in liquid oxygen flow [5, 6]. With the help of these data, the heating of the fuel cryogenic component at the inlet of the main oxidizer pump and the malleability of the vapor condensation zone have been determined:

$$\frac{\partial V_g}{\partial p_l} \approx S_g d_g \left[-0{,}0091\alpha^{-1{,}7} K^{1{,}67} \frac{\partial \alpha}{\partial p_l} + \right.$$

$$\left. + 0{,}0217\alpha^{-0{,}7} K^{0{,}67} \frac{\partial K}{\partial p_l} \right],$$

where p_l is the pressure in the liquid oxygen flow; V_g is the condensation zone v lume; d_g, S_g are the diameter of the hole and the total area of the holes through which gaseous oxygen is blown; α is the ratio of the liquid oxygen axial velocity to the gaseous oxygen axial velocity; K is phase transition criterion, the value of which is calculated according to the formula

$$K = \frac{L}{C_l \Delta T_l},$$

where $\Delta T_l = T_{ls} - T_l$ is the underheating of the liquid to the saturation state; T_{ls} is the saturation temperature (at a given pressure in the liquid); T_l is the temperature of the liquid; C_l is heat capacity of the liquid; L is the specific heat of condensation.

Unlike the pumps used in various industries, the LRE pumps are designed and manufactured with high anti-cavitation properties. In particular, this means that the LRE pumps have a lower breakdown pressure in the second critical mode, but at the same time, cavitation bubbles appear in them at higher inlet pressures. The modern LRE pumps at all stages of operation (engine start, main mode, stop) operate in the cavitation mode [7]. In this regard, taking into account cavitation phenomena in the LRE pumps is of crucial importance.

The most developed mathematical model of cavitation oscillations in a hydraulic system with screw centrifugal pumps for LREs is hydrodynamic model [8] with generalized experimental and calculation coefficients [9, 10], which contains the equation of the dynamics of cavitation caverns in terms of the pressure at the pump inlet and the equation for determining the pressure at the pump outlet:

$$(1 + \alpha_p)\frac{dp_1}{dt} = \frac{G_1 - G_2}{C_K} + R_{K1}\frac{Gd_1}{dt} + R_{K2}\frac{Gd_2}{dt},$$

$$p_2 = p_1 + p_H \cdot \breve{p}_H(V_K) - J_H \frac{Gd_2}{dt},$$

where p_1, G_1 are the pressure and the fluid flow (consumption) at the pump inlet; p_2, G_1 are the pressure and the fluid flow at the pump outlet; p_H, $\breve{p}_H(V_K)$ are the pressure and the cavitation function of the pump; V_K is the volume of cavitation caverns; J_H is coefficient of inertial resistance of the liquid in the flow part of the pump; $\alpha_p = \frac{\partial(B_1 T_K)}{\partial p_1}(G_1 - G_2)$; $C_K = -\frac{\gamma}{B_1}$ is the malleability of caverns; R_{K1}, R_{K2} are the cavitation resistance coefficients B_2: $R_{K1} = B_2 - \frac{B_1 \cdot T_K}{\gamma} + \frac{\partial p_{CP}}{\partial G_1} - \frac{\partial(B_1 T_K)}{\partial G_1}(G_1 - G_2)$, $R_{K2} = \frac{B_1 \cdot T_K}{\gamma}$; $B_2(p_1, G_1) = \frac{\partial p_1}{\partial G_1}$; B_1, T_K are the elasticity and the time constant of cavitation caverns; γ is the specific gravity of liquid; p_{CP} is the pump failure pressure.

The oxidizer feed system of the *Cyclone-4M* first stage sustainer engine contains extensive branched pipelines. For mathematical modeling of the low-frequency dynamics of such feed systems, methodological approach [11] can be recommended. It involves the sequential solution of the following problems: to build a linear mathematical model of the dynamics of the hydraulic tract that is considered a system with distributed parameters and to determine its frequency characteristics; to replace this system by a system with lumped parameters, which is built from finite hydrodynamic elements based on matching the frequency characteristics of these two systems; to build a non-linear mathematical model of the low-frequency dynamics of the hydraulic tract for the calculation of the transient processes during the engine start.

Mathematical modeling of fluid dynamics in a cylindrical homogeneous pipeline that considered a system with distributed parameters is based on the use of the equations of unsteady fluid motion, the equation of discontinuity, and the equation of state [12], [13]. At the same time, the fluid dynamics are described by the following system of partial differential equations:

$$\begin{cases} \frac{\partial p}{\partial z} + \frac{1}{g \cdot F} \cdot \frac{\partial G}{\partial t} + \frac{k}{g \cdot F} \cdot G = 0, \\ \frac{\partial G}{\partial z} + \frac{g \cdot F}{c^2} \cdot \frac{\partial p}{\partial t} = 0, \end{cases}$$

where p, G are the pressure and the mass per second flow of liquid; z is coordinate of the axis of the trunk; F is the cross-sectional area of the trunk;

ISSN 2409-9066. Sci. innov. 2022. 18 (6)

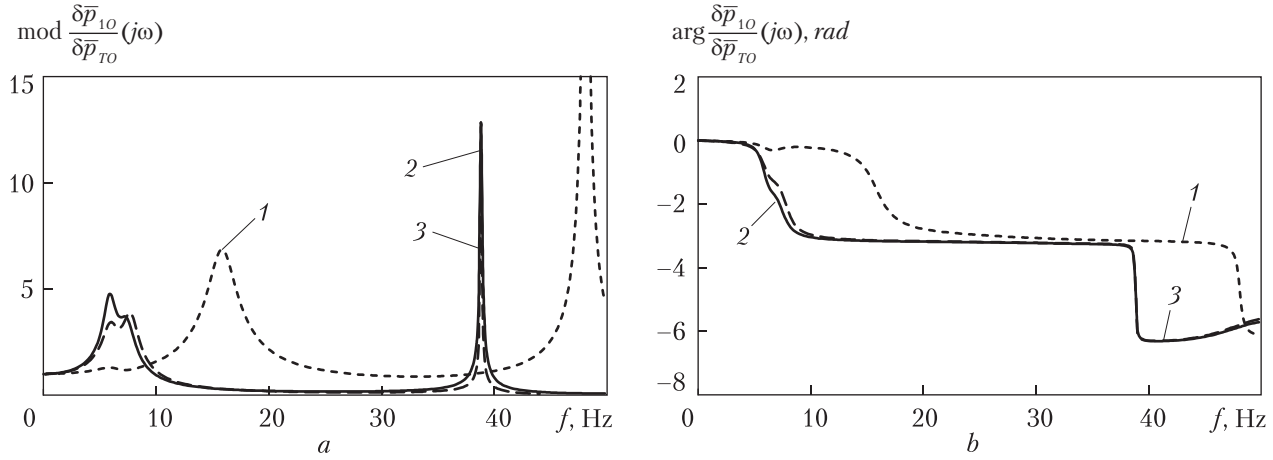

Fig. 2. The amplification factor of the oxidizer feed line of the *Cyclone*-4M first stage multi-engine propulsion system (*a* — module; *b* — argument): *1* — cavitation in the pumps neglected, distributed parameters of the feed system; *2* — given cavitation in pumps, with distributed parameters of the feed system; *3* — given cavitation in pumps, with lumped parameters of the feed system

k is the reduced coefficient of linear friction per unit of the trunk length; g is the acceleration of gravity; c is the speed of sound in the liquid that flows through a pipeline with elastic walls.

The pipeline as a system with lumped parameters can be represented in the form of a quadripole:

$$\begin{cases} \delta\overline{p}_2 = \delta\overline{p}_1 - (R + sJ)\cdot\delta\overline{G}_1 \\ \delta\overline{G}_2 = -Cs\cdot\delta\overline{p}_1 + \delta\overline{G}_1 \end{cases}$$

where R, J are the coefficients of linearized hydraulic resistance and inertial resistance of the pipeline section; C is the lumped malleability of the pipeline section; s is the Laplace variable.

Coefficients R and J are determined by the geometry of the pipeline, pressure losses and fluid flow. The number of lumped malleability values C and their values are chosen based on the required accuracy of matching in the specified frequency range of the considered frequency characteristics of the pipeline as a system with distributed and lumped parameters.

Figure 2 presents the coefficients of amplification of the oxidizer feed pipeline by pressure in the section from the oxidizer tank (oxidizer pressure in the tank p_{TO}) to the inlet of the oxidizer booster pump (pressure at the booster inlet p_{1O}), both without taking into account and given the cavitation in the pumps; the calculations have been made for the cases when the pipeline is considered a system with distributed parameters (curve 2) and a system with lumped parameters (curve 3). This figure demonstrates a satisfactory match between the amplification of the pipeline as a distributed parameter system and the pipeline as a lumped parameter system. In addition, there is a significant influence of cavitation in pumps on the natural frequencies of oscillations in the oxidizer feed system. Thus, because of cavitation in the LRE pumps, the first natural frequency of liquid oscillations in the oxidizer line decreases almost three times, from 15.8 Hz to 5.8 Hz.

The controller of fuel flow to the gas generator is of decisive importance for setting and keeping of the necessary power of the turbopump unit and, therefore, the thrust of the engine. Therefore, the spread of the design and mode parameters of the flow controller can significantly affect the thrust spread of the LRE in the course of its start. For mathematical modeling of dynamic processes in the fuel consumption controller at start, a mathematical model described in [14] has been developed. The equation of motion of the moving parts of the flow controller is written as follows:

$$m_P\frac{d^2x}{dt^2} + F_{FR}(x) + k_{SP}\,x = F_P(p_A - p_B) - R^O_{SP} + R_{HD},$$

where m_p is the mass of moving parts of the flow controller; x is the displacement of the flow controller spool; $F_{FR}(x)$ is the force of friction, proceeding from the hypothesis of dry friction; k_{SP} is the spring stiffness coefficient; F_P is the cross-sectional area of the spool; p_A, p_B are the fluid pressure in cavities A and B, respectively (see [14]); R_{SP}^O is the initial tightening of the flow controller spring; R_{HD} is the hydrodynamic force.

The static characteristic of the flow controller $G_{FR} = G_{FR}(\Delta p_{FR})$, which is a measure of the static accuracy of the controller, can be presented in a parametric form (parameter x), with liquid leaks neglected, by the following ratios:

$$G_{FR}^2 = \frac{2g\gamma_F (R_{SP}^O + k_{SP}x)}{\frac{F_P}{(\mu_1 F_1)^2} + \frac{\delta_{ED}\, l_Z(x)\, k_{HD}}{(\mu_2 F_2(x))^2}},$$

$$\Delta p_{FR} = G_{FR} \frac{1}{2g\gamma_F} \left(\frac{1}{(\mu_1 F_1)^2} + \frac{1}{(\mu_2 F_2(x))^2} \right),$$

where δ_{ED} is the thickness of the spool edge; $l_Z(x)$ is the total length of the edges of the spool windows; k_{HD} is empirical coefficient; γ_F is the fuel specific gravity; $\mu_1 F_1$ is the effective area of the controller measuring throttle windows; $\mu_2 F_2(x)$ is the effective area of the spool windows.

In the elements of the gas tract of the RD-870 LRE (the combustion chamber, the gas generator, and the gas pipe), the gas flows under the supply of heat released from fuel combustion. In the general case, the gas flow is described by the differential equations in partial derivatives, which express the laws of conservation of mass, momentum, and energy, and the equation of state for gas [12], [4]. In practice, the principle of regulating the range of model dynamics is used in mathematical modeling of dynamic processes in LRE [15]. The regulation of the dynamic range of the model allows us to use different principles for model building and methods for its study in different frequency ranges, which greatly simplifies the modeling process. In particular, in the low-frequency range, the engine combustion chamber, the gas generator, and the gas pipelines can be considered elements with lumped parameters, since their linear dimensions are significantly smaller as compared with the length of the acoustic wave [15].

The working process in the combustion chamber and in the gas generator is a sequence of physical and chemical processes (injection of liquid components of fuel, its atomization, crushing, formation of droplets, evaporation, mixing, ignition, burning) that result in the transformation of fuel into final products of combustion. Because of the complexity of these processes and their interrelationships, a general theory of the working process in the LRE chamber has not yet been created, and quantitative studies allow only highlighting the main phenomena and building a simplified model of the processes [16]. The real process of combustion of liquid fuel components is difficult to describe analytically, and its main characteristic — the fuel burnout curve — depends on many factors and can be complex. M.S. Natanzon has proposed, when modeling low-frequency processes in LRE, to replace the real burn-up curve with a single step function — pure (transport) delay $\varphi_c(t) = 1(t - \tau_c)$, where τ_c is the time of transformation of liquid fuel components into combustion products [12], [17]. Despite the fact that this model is quite approximate, it is widely used until now (e.g., [18], [19]). The transport delay is also approximated by the temperature transfer curve by turbulent mass flows in the elements of the gas tract: $\varphi_s(t) = 1(t - \tau_s)$, where τ_s is the time of gas stay in the section of the tract [12], [18].

In [20]—[22], schemes of approximate replacement of the delay link equation $y(t) = x(t - \tau)$ by systems of ordinary differential equations have been proposed. These schemes are based on the approximation of the transfer function of delay link $W_e(p\tau) = \exp(-p\tau)$ by rational functions of $p\tau$ (here p is the complex variable of the Laplace transform at zero initial conditions; τ is the delay time). It has been shown that for small values τ (such as the time of transformation of fuel liquid components into combustion products), the fractional Taylor series of the 1st order can be used as

ISSN 2409-9066. Sci. innov. 2022. 18 (6)

an approximating rational function. The two rational functions are recommended for approximating the transfer functions of the delay links in the dynamics equations of the gas generator and gas pipeline (with delays τ_{II}): function $R_{n(T02)}(p\tau) = [T_{0,2}(p\tau/2)]^2 = 1/(1 + p\tau/2 + 0{,}125p^2\tau^2)^2 \approx W_e(p\tau)$ that is obtained by replacing the delay link with a chain of two oscillating links with half the delays [21] and function $W_e(p\tau) \approx P_{1,2}(p\tau) = (1 - p\tau/3) / (1 + 2p\tau/3 + p^2\tau^2/6)$ built with the use of the Padé method [22]. The approximation with functions $R_{n(T02)}(p\tau)$ and $P_{1,2}(p\tau)$ allows obtaining acceptable results of LRE start calculations for values $\omega\tau \le 3$ (where ω is the angular frequency of characteristic oscillations).

EXTERNAL AND INTERNAL FACTORS OF RD-874 MULTI-ENGINE

Each rocket engine is unique in terms of its characteristics, design solutions, features of the process in the main and transitional modes and many other parameters. The list of internal factors for each engine due to its characteristics is also unique. This list usually includes the following [23]: change in the hydraulic resistance of the paths to the gas generator and the combustion chamber, fluctuations in the diameter of the critical section of the combustion chamber, deviation of the diameter of the critical sections of the turbine nozzles. This list can be extended by divergence of turbine and pump efficiency, deviations of oxidizer and fuel pump pressures, temperature fluctuations in the fire spaces of the gas generator and the combustion chamber.

The thrust spread at the engine start is also affected by different time of opening the oxidizer and the fuel valves on the gas generator and the combustion chamber. In addition, the dynamic characteristics of the LRE start are affected by the spread of the coefficients of the mathematical model of the dynamic processes at start: the delay time of gas formation in the gas generator, the time of stay of combustion products in the gas generator and gas pipeline, the coefficients of fluid malleability in the oxidizer and fuel hydraulic paths.

The given list of the internal factors may be extended further. The full list can be very cumbersome, which significantly complicates the determination of the influence of internal factors on the thrust spread. However, it should be noted that among all internal factors, one can single out those that have a weak (as compared with others) influence on the thrust spread at the start. In the first approximation, such factors can be ignored. In order to determine the internal factors that have the greatest influence on the thrust spread at the start, it is necessary to conduct a series of preliminary calculations of engine start, in which the internal factors are alternately varied within their spreads and the deviations of the studied parameters, for example, the time of reaching 90% thrust are determined. Below, we consider the internal factors with the largest deviations.

The list of the internal factors that have the greatest influence on the thrust spread of the RD-874 multi-engine propulsion system at its start, as well as the limits of variation of their values are given in Table 1. Nine factors from this Table determine the static characteristics of the engine and affect both the time of 90 % thrust takeoff and the engine thrust in steady state of operation. Two factors (the time the combustion products stay in the gas generator and the opening time of the fuel valve on the gas generator) affect only the time during which the engine reaches 90% thrust.

The external factors of the RD-874 multi-engine propulsion system should include the propellant temperature and the pressure at the pump (engine) inlets.

Method for setting the spread of the external and the internal factors

Let us assume that the mathematical model of the low-frequency dynamic processes of the start of RD-874 multi-engine propulsion system contains n external and internal factors $\alpha_1, ..., \alpha_n$ that have the greatest influence on the thrust spread of the multi-engine propulsion system at its start. The set of points Ai with Cartesian coordinates $\alpha_{1,i}, ...,$

$\alpha_{n,i}$ forms a n-dimensional space of parameters. In fact, the parameters $\alpha_1, ..., \alpha_n$ vary within limited ranges and belong to admissible set **P** that is a n-dimensional region of the parameter space:

$$\mathbf{P} = \{\alpha_1, ..., \alpha_n : \alpha_j^{\min} \le \alpha_j \le \alpha_j^{\max}, j = 1, ..., n\}. \quad (1)$$

A direct approach to determining the thrust spread of the RD-874 multi-engine propulsion system during its start is to implement various combinations of external and internal factors from admissible set (1). The values of imprecisely specified parameters (trial points) can be chosen based on a random search. The more uniformly the values of external and internal factors are located in the parameter space, the more effective is search [24]. In both cases, the solution to the problem of determining the thrust spread at the start of the RD-874 multi-engine propulsion system, which is caused by the spread of the external and the internal factors, requires a large amount of calculations and is quite time-consuming even with a relatively small number of varying parameters.

In this research, for the selection of trial points $\alpha_1, ..., \alpha_n \in \mathbf{P}$, we propose using the method for probing the space, which is called the LP-search. This method is implemented for a unit n-dimensional cube K^n. The points of LP_τ-sequences (Sobol sequences) are used as trial points in the n-dimensional cube. The LP_τ-sequences are the most evenly distributed among all currently known sequences. Their use has an advantage as compared with the simplest random search and is much more effective than the uniform cubic lattices at $n > 1$ [24].

Different combinations of deviations of each of the external and internal factors determine different combinations of the varying parameters for the calculations of the start. The combinations of deviations of parameters reduced to a dimensionless form have been determined by LP_τ-sequences built in a unit cube K^n according to [24]. The use of LP_τ-sequences makes it possible to cover the deviations of the external and internal factors in the most uniform manner with a smaller number of realizations. The calculation algorithm has been presented in [24]. Tables 2 and 3 contain a set of combinations of the external and internal factors of the RD-874 multi-engine propulsion system, which are obtained with the use of the LP_τ-sequence. Each line of Tables determines coordinates $(x_1, x_2, ..., x_n)$ of a point in the n-dimensional unit cube and specifies one of the options for realizing the deviations of the external and internal factors. Each column of the Table specifies one coordinate x_i of a point in the n-dimensional unit cube for all options of the realization of deviations of the external and internal factors.

Table 1. **The Internal Factors of the Engines of RD-874 Multi-Engine Propulsion System**

No.	Factor	Range of variation, %	Engine No.1	Engine No.2	Engine No.3	Engine No.4
1	Temperature in the gas generator	±3.9	x_1	x_{12}	x_{23}	x_{34}
2	Temperature in the combustion chamber	±3.4	x_2	x_{13}	x_{24}	x_{35}
3	Area of the nozzles of the turbine	±2	x_3	x_{14}	x_{25}	x_{36}
4	Turbine efficiency	±5	x_4	x_{15}	x_{26}	x_{37}
5	Oxidizer pump pressure	±2	x_5	x_{16}	x_{27}	x_{38}
6	Oxidizer pump efficiency	±1.3	x_6	x_{17}	x_{28}	x_{39}
7	The pressure of the fuel pump of the first stage	±2	x_7	x_{18}	x_{29}	x_{40}
8	Efficiency of the fuel pump of the first stage	±3	x_8	x_{19}	x_{30}	x_{41}
9	Residence time of combustion products in the gas generator	±20	x_9	x_{20}	x_{31}	x_{42}
10	Initial compression of the fuel flow controller spool spring	±10	x_{10}	x_{21}	x_{32}	x_{43}
11	Opening time of the fuel valve on the gas generator	±20	x_{11}	x_{22}	x_{33}	x_{44}

ANALYSIS OF THE RESULTS OF DETERMINING THE THRUST SPREAD OF *CYCLONE-4M* FIRST STAGE MULTI-ENGINE PROPULSION SYSTEM AT ITS START

Using the mathematical model of the start of the *Cyclone-4M* first stage multi-engine propulsion system, which is presented conceptually in this research, in accordance with the above-described method of uniform assignment of deviations of the external and internal factors, we have made a series of calculations of the start of the RD-874 multi-engine propulsion system. When marking the four engines of the RD-874 multi-engine propulsion system, we assume that the set of internal factors (parameter deviations) of engine No. 1 corresponds to the set of coordinates (x_1, x_2, ..., x_{11}), that of engine No. 2 corresponds to (x_{12}, x_{13}, ..., x_{22}), that of engine No. 3 corresponds to (x_{23}, x_{24}, ..., x_{33}), and that of engine No. 4 corresponds to (x_{34}, x_{35}, ..., x_{44}), in accordance with Table 1. Figures 3 and 4 show the time dependences of the combustion chamber pressure at the start of the RD-874 multi-engine propulsion system, which are calculated on the condition that the spread of the internal factors for all RD-870 engines is the same and equal to that for engine No. 1. In this case, the set of the internal factors is as follows: $x_1 = x_{12} = x_{23} = x_{34}$, $x_2 = x_{13} = x_{24} = x_{35}$ ... x_{11}, $= x_{22} = x_{33} = x_{44}$ (see Table 1).

Figures 3 and 4, curves 1 and 2 show the lower and the upper envelopes of the combustion chamber pressure. Curves 3 and 4 in Fig. 3 feature the dependencies obtained in the calculation options with the minimum (No. 176) and maximum (No. 191) time of 90% thrust takeoff. Curves 3 and 4 in Fig. 4 show the dependencies obtained in the calculation options with the minimum (No. 176) and the maximum (No. 247) combustion chamber pressure. From these Figures and Tables 4 and 5, it can be seen that the spread of the external and internal factors may lead to a significant difference in the time of reaching 90% thrust at the engine start (more than 0.08 s) and a significant thrust spread at steady state (7% and more as compared with its nominal value). At the same time, it is impossible to single out the two worst options of the combinations of the spread of these factors, which would determine the lower and the upper envelopes for the family of calculated time dependences of the combustion chamber pressure,

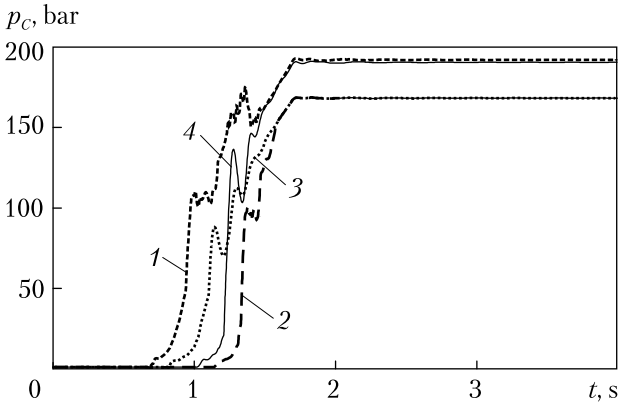

Fig. 3. The calculated time dependences of the combustion chamber pressure at the start of the RD-874 multi-engine propulsion system (the spread of the internal factors in all RD-870 engines is the same) for the options in which the minimum and the maximum time of 90% thrust takeoff is realized: *1, 2* — the lower and the upper envelopes; *3* — the minimum time of thrust takeoff (option No. 176); *4* — the maximum time of thrust takeoff (option No. 191)

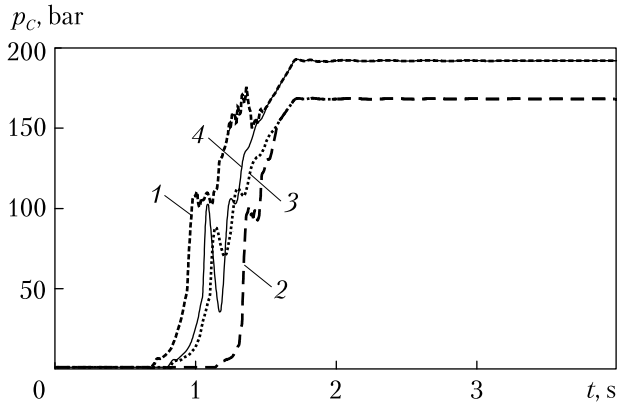

Fig. 4. The calculated time dependences of the combustion chamber pressure at the start of the RD-874 multi-engine propulsion system (the spread of the internal factors in all RD-870 engines is the same) for the options in which the minimum and the maximum thrust is realized: *1, 2* — the lower and the upper envelopes; *3* — the minimum thrust (option No. 176); *4* — the maximum thrust (option No. 247)

which are obtained upon considering all the options of the spread of the external and internal factors.

When realizing the spread of external and internal factors according to option No. 176 (see Tables 2 and 3), internal factors x_1, x_4, x_6, x_7, and x_{10} take values close to their limit ones (less than 10% of the limit value). For options No. 191 and No. 247, such values are taken by the internal factors x_1, x_4, x_9 and, respectively, x_1, x_4, x_8, and x_{10}. When the number of internal factors is not very large (in our case, 11), this information allows us to find out which internal factors are responsible for the largest deviation of the studied parameter (in our case, the combustion chamber pressure).

In this research, the calculated time dependences of the pressure in the combustion chamber at the start of the RD-874 multi-engine propulsion system with the same spread of the external and internal factors in all RD-870 engines are the starting point that allows us to assess the degree of influence of inevitable spread of the engine geometric and mode parameters on the start characteristics of the RD-874 multi-engine propulsion system consisting of four RD-870 engines.

The further calculations of the start of the RD-874 multi-engine propulsion system have been made with different spreads of the external and internal factors for all four engines. The results of these calculations have shown that the lower and upper envelope curves for the time dependences of the combustion chamber pressure, which are calculated for each of the four engines (No. 1, No. 2, No. 3, and No. 4), are close to the similar envelope curves obtained in the case when the spread of the parameters in all engines is the same (see Figs. 3 and 4). In addition, the minimum and the maximum values of the time of reaching 90% thrust and the time of complete thrust takeoff for all engines are also close (see Tables 4 and 5).

It is very important from a scientific point of view, as well as for practical use, that the minimum and maximum values of the time of reaching 90% thrust in the entire RD-874 multi-engine propulsion system range within (–0.0490 s, +0.0328 s)

Table 2. **A Set of Combinations of the Internal Factors of the RD-874 Multi-Engine Propulsion System**

Option No.	Coordinates of LP_τ sequence points											
	Engine No. 1			Engine No. 2			Engine No. 3			Engine No. 4		
	x_1	...	x_{11}	x_{12}	...	x_{22}	x_{23}	...	x_{33}	x_{34}	...	x_{44}
1	0.5	...	0.5	0.5	...	0.5	0.5	...	0.5	0.5	...	0.5
2	0.25	...	0.25	0.75	...	0.75	0.25	...	0.25	0.25	...	0.25
3	0.75	...	0.75	0.25	...	0.25	0.75	...	0.75	0.75	...	0.75
4	0.125	...	0.875	0.875	...	0.375	0.375	...	0.125	0.125	...	0.875
5	0.625	...	0.375	0.375	...	0.875	0.875	...	0.625	0.625	...	0.375
6	0.375	...	0.625	0.125	...	0.625	0.125	...	0.375	0.375	...	0.625
7	0.875	...	0.125	0.625	...	0.125	0.625	...	0.875	0.875	...	0.125
8	0.063	...	0.688	0.313	...	0.188	0.938	...	0.938	0.063	...	0.188
9	0.563	...	0.188	0.813	...	0.688	0.438	...	0.438	0.563	...	0.688
10	0.313	...	0.938	0.563	...	0.938	0.688	...	0.688	0.313	...	0.438
11	0.813	...	0.438	0.063	...	0.438	0.188	...	0.188	0.813	...	0.938
12	0.188	...	0.313	0.688	...	0.313	0.563	...	0.813	0.188	...	0.813
...	...	...	...	...	...	...	...	...	...	...	...	...
255	0.996	...	0.332	0.043	...	0.793	0.746	...	0.254	0.395	...	0.051
256	0.002	...	0.803	0.455	...	0.037	0.486	...	0.881	0.447	...	0.557

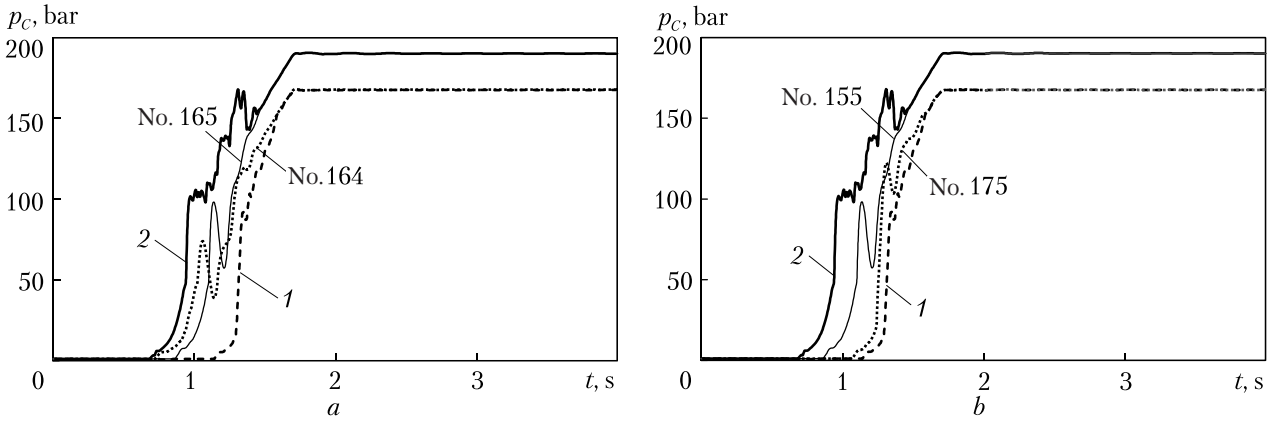

Fig. 5. The calculated time dependences of the combustion chamber pressure at the start of engine No. 3 for the calculation options in which the minimum and the maximum time of 90% thrust takeoff (*a*) and the minimum and the maximum thrust (*b*) are realized: *1* — the lower envelope; *2* — the upper envelope

that is significantly smaller (approximately 2 times) than the corresponding ranges of the time of reaching 90% thrust for each individual engine (see Table 4). The thrust spread of the entire RD-874 multi-engine propulsion system is also significantly less than that of one engine. As can be seen from Table 5, the minimum and the maximum spread of the pressure in the combustion chamber range from –3.34% to +3.23% of the engine nominal thrust (calculated per engine).

Based on the results of the calculations, it has been established that all engines have different combination of spreads of the external and internal factors, which leads to the largest deviation of the combustion chamber pressure from the nominal one. The largest deviation of the time of reaching 90% thrust has been obtained for the following combinations of the external and internal factors:

- for engine No. 1: No. 176 (min) and No. 25 (max);
- for engine No. 2: No. 164 (min) and No. 173 (max);
- for engine No. 3: No. 164 (min) and No. 165 (max);
- for engine No. 4: No. 250 (min) and No. 207 (max).

The largest deviation of the thrust takeoff from the nominal value has been obtained for the spread of the parameters, which corresponds to the following options:

- No. 176 (min), No. 247 (max), for engine No. 1;
- No. 164 (min), No. 78 (max), for engine No. 2;
- No. 175 (min), No. 155 (max), for engine No. 3;
- No. 5 (min), No. 187 (max), for engine No. 4.

Figure 5 shows the calculated time dependences of the combustion chamber pressure at the start of engine No. 3, as an example of the calcula-

Table 3. **A Set of Combinations of the External Factors of the RD-874 Multi-Engine Propulsion System**

Option No.	Coordinates of LP_τ sequence			
	Oxidizer pressure	Oxidizer temperature	Fuel pressure	Fuel temperature
	x_{45}	x_{46}	x_{47}	x_{48}
1	0.5	0.5	0.5	0.5
2	0.25	0.75	0.25	0.75
3	0.75	0.25	0.75	0.25
4	0.875	0.875	0.125	0.375
5	0.375	0.375	0.625	0.875
6	0.625	0.125	0.375	0.625
7	0.125	0.625	0.875	0.125
8	0.188	0.438	0.563	0.313
9	0.688	0.938	0.063	0.813
10	0.438	0.688	0.813	0.563
11	0.938	0.188	0.313	0.063
12	0.813	0.563	0.688	0.188
...	...	...	...	...
255	0.582	0.098	0.949	0.84
256	0.979	0.541	0.389	0.588

tion options in which the largest deviations of the time of reaching 90% thrust and the thrust takeoff are realized.

In general, for the RD-874 multi-engine propulsion system, the largest deviations of the time of reaching 90% thrust and the thrust spread have been obtained for options No. 147 (min) and No. 251 (max). The transient processes during the start of the RD-874 multi-engine propulsion system, as calculated for these options of the spread of parameters, are presented in Fig. 6. These calculated time dependences of the combustion chamber pressure at the start are quite different and difficult to predict.

The estimated spread of the time of reaching 90% thrust and the thrust spread of the RD-874 multi-engine propulsion system are pseudo-random values. To make sure that they obey the normal distribution law, the consistency of the obtained statistical and assumed theoretical (normal) distributions has been assessed with the use of Pearson's chi-squared test χ^2. For this purpose, the obtained samples of the time of reaching 90% thrust and the thrust takeoff of the multi-engine propulsion system at steady state are placed in 8 digits, and the histograms are constructed for the two cases: with the same parameter deviations in all four engines (see Fig. 7, curve 1) and for the engine propulsion system as a whole with various deviations of engine parameters (see Fig. 7, curve 3). The theoretical probability of a random value falling into an arbitrary category (curves 2 and 4, Fig. 7), as is usually accepted [25], has been estimated with the use of experimental statistical characteristics: mathematical expectation $\widehat{M}$ and variance $\widehat{D}$. The critical value χ^2 for the presented

Table 4. **Limit Deviations of the Time of 90 % Thrust Takeoff from the Nominal Value (min is the largest deviation towards minimum, max is the largest deviation towards maximum)**

	Option	Time deviation, s	
		min	max
1	Spread of the parameters of all engines is the same	–0.0878	+0.0741
2	Spread of the parameters is different, engine No. 1	–0.0899	+0.0840
3	Spread of the parameters is different, engine No. 2	–0.0925	+0.0692
4	Spread of the parameters is different, engine No. 3	–0.0873	+0.0609
5	Spread of the parameters is different, engine No. 4	–0.0800	+0.0601
6	Spread of the parameters is different, RD-874 multi-engine propulsion system	–0.0490	+0.0328

Table 5. **Limit Deviations of the Pressure Takeoff from the Nominal Value (min is the largest deviation towards minimum, max is the largest deviation towards maximum)**

	Option	Deviation of the pressure in the combustion chamber, %	
		min	max
1	Spread of the parameters of all engines is the same	–6.21	+7.02
2	Spread of the parameters is different, engine No. 1	–6.22	+7.01
3	Spread of the parameters is different, engine No. 2	–6.79	+6.33
4	Spread of the parameters is different, engine No. 3	–6.57	+5.99
5	Spread of the parameters is different, engine No. 4	–5.57	+5.51
6	Spread of the parameters is different, RD-874 multi-engine propulsion system	–3.34	+3.23

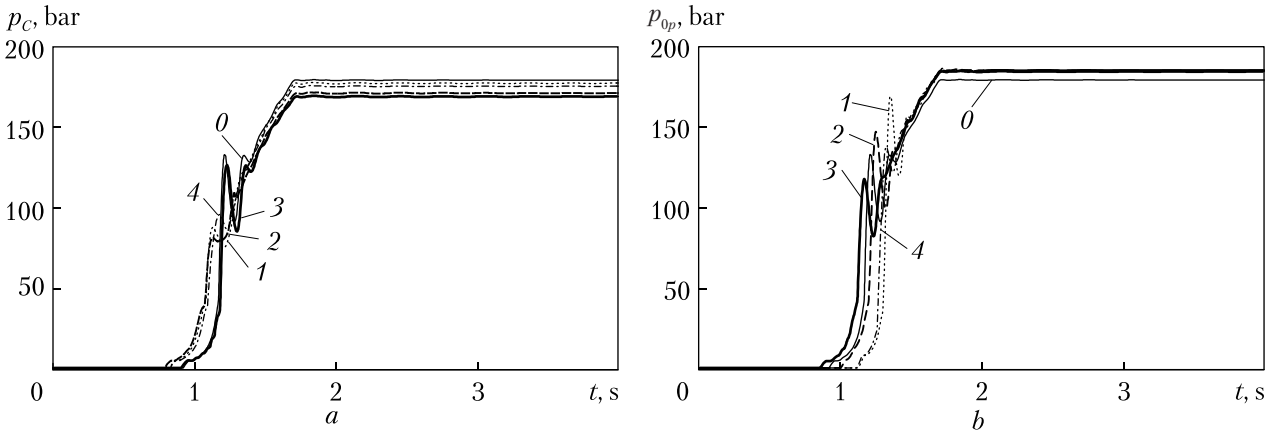

Fig. 6. The calculated time dependences of the combustion chamber pressure at the start of the RD-874 multi-engine propulsion system for option No. 147 in which the time of reaching 90% thrust and the thrust of the entire propulsion system are minimum (*a*) and for option No. 251 in which the time of reaching 90% thrust and the thrust of the entire propulsion system are maximum (*b*): *0* — the nominal mode; *1, 2, 3, 4* — calculations for engines No. 1, 2, 3, and 4, respectively

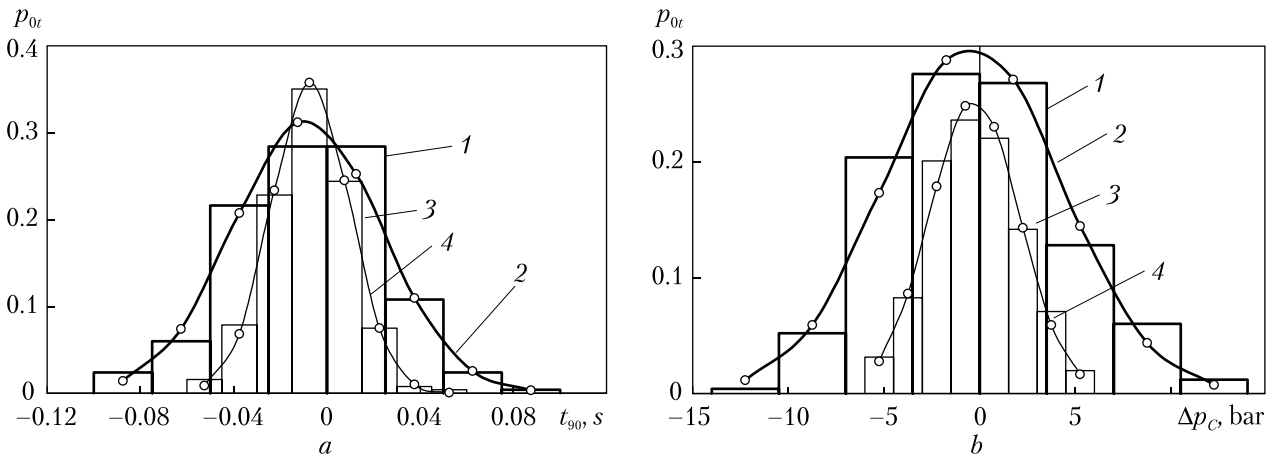

Fig. 7. Statistical and theoretical distributions of the spread of the time of reaching 90% thrust (*a*) and the combustion chamber pressure (*b*) for the case of the same parameter deviations in all engines (curves *1, 2*) and for the propulsion system as a whole (curves *3, 4*): *1, 3* — statistical distributions; *2, 4* — theoretical distributions

histograms is $\chi^2_{kp} = 11.1$. All calculated values χ^2 for the specified data do not exceed the critical value, which confirms the hypotheses about the consistency of the statistical and theoretical distributions both for the time of reaching 90% thrust and for the thrust of the propulsion system at steady state.

Figure 7 clearly illustrates that the spread of the time of reaching 90% thrust and the thrust spread for the entire RD-874 multi-engine propulsion system is significantly smaller (about 2 times) than the spread of the time of reaching 90% thrust and the thrust spread of each individual engine.

It has been shown that the experimental mathematical expectations for all samples, as expected, are close to zero. The experimental variances of individual engines are 0.001 s, for the spread of the time of reaching 90% thrust , and 11.7% of the nominal thrust of the engine, for the thrust spread. For the multi-engine propulsion system as a whole, the experimental variances are significantly

smaller: 0.0003 s, for the spread of the time of reaching 90% thrust , and 3.0% of the nominal thrust of the engine, for the thrust spread.

CONCLUSIONS

The nonlinear mathematical model of the start of the *Cyclone-4M* 1st stage RD-874 multi-engine propulsion system has been developed. It describes the low-frequency dynamics of the modules and systems of the engine propulsion system and allows taking into account the influence of the spread of the internal and external factors on the transient processes in the multi-engine propulsion system during the start.

The method for determining the thrust spread caused by the internal and external factors during the start of the *Cyclone-4M* first stage multi-engine propulsion system has been developed. It is based on the use of LP_τ-uniformly distributed sequences and is much more efficient as compared with the random search.

For each engine that is part of the engine propulsion system, 11 internal factors that have the greatest influence on the thrust spread have been determined. Respectively, for the entire engine propulsion system, there are 44 internal factors.

Based on the results of the calculations, the transient processes in the RD-874 multi-engine propulsion system at various combinations of the external and internal factors have been determined, and the lower and upper envelope curves have been built for the time dependences of the pressure in the combustion chamber for each LRE included in the multi-engine propulsion system. It has been established that the envelope curves of the combustion chamber pressure dependences, which are built under the condition of the same and different spreads of the internal factors for all RD-870 engines, have close values.

It has been shown that the spread of the time of reaching 90% thrust and the thrust spread for the RD-874 multi-engine propulsion system as a whole is significantly (approximately 2 times) smaller than those for each individual RD-870 engine. The time spread ranges from 0.0490 s to +0.0328 s, while the thrust spread ranges from 3.34 % to +3.23 % of the nominal thrust.

The consistency of the obtained statistical and theoretical distributions has been assessed with the use of Pearson's chi-squared test χ^2. It has been shown that all calculated values χ^2 do not exceed its critical value, which confirms the hypotheses about the normal law of the distribution of the spread of the time of reaching 90% thrust and the thrust spread at steady state.

The research funding. *The research is funded within the framework of the innovation project approved by the Presidium of the NAS of Ukraine (order No. 31 dated 20.01.2021), under Contract II-5-21 dated February 1, 2021, made between the National Academy of Sciences of Ukraine, the Institute of Technical Mechanics of the NAS of Ukraine, and the State Space Agency of Ukraine (State Register No. 0121U107999).*

REFERENCES

1. Nationwide targeted scientific and technical space program of Ukraine for 2021—2025. http://materialy.kmu.gov.ua/af3b841c/docs/2b0a8327/Dodatok.pdf (Last accessed: 09.02.2022).
2. Space rocket complexes. Cyclone-4M launch vehicle. http://www. https://www.yuzhnoye.com/ua/technique/launch-vehicles/launch-vehicles/cyclone-4m/ (Last accessed: 09.02.2022).
3. Pylypenko, O. V., Prokopchuk, A. A., Dolgopolov, S. I., Pisarenko, V. Yu., Kovalenko, V. N., Nikolayev, O. D., Khoryak, N. V. (2017). Pequliarities of mathematical modeling of low-frequency dynamics of the staged liquid rocket sustainer engines at its startup. *Space Sci.&Technol.*, 23(5), 3—13 [in Russian]. https://doi.org/10.15407/knit2017.05.003
4. Shevyakov, A. A., Kalnin, V. M., Naumenkova, M. V., Dyatlov, V. G. (1978). *Theory of Rocket Engine Automatic Control.* Moscow: Mashinostroyeniye [in Russian].
5. Pilipenko, V. V., Dorosh, N. L., Man'ko, I. K. (1993). Experimental investigations of steam condensation when a gaseous oxygen jet is blown into a liquid oxygen flow. *Technical mechanics*, 2, 77—80 [in Russian].

6. Dorosh, N. L. (2020). Modeling of condensation of an oxygen vapor jet in liquid oxygen. *Applied problems of mathematical modeling*, 3(2.2), 149—155 [in Ukrainian]. https://doi.org/10.32782/KNTU2618-0340/2020.3.2-2.14
7. Borovsky, B. I., Ershov, N. S., Ovsyannikov, B. V., Petrov, V. I., Chebaevsky, V. F., Shapiro, A. S. (1975). *High-speed vane pumps*. Moskow: Mashinostroenie [in Russian].
8. Pilipenko, V. V., Zadontsev, V. A., Natanzon, M. S. (1977). *Cavitation oscillations and dynamics of hydraulic systems*. Moscow: Mashinostroenie [in Russian].
9. Pilipenko, V. V., Dolgopolov, S. I. (1998). Experimental and computational determination of the coefficients of the equation for the dynamics of cavitation cavities in inducer centrifugal pumps of various sizes. *Technical mechanics*, 8, 50—56 [in Russian].
10. Pylypenko, O. V., Dolhopolov, S. I., Nikolayev, O. D., Khoriak, N. V. (2020). Mathematical simulation of the start of a multiengine liquid-propellant rocket propulsion system. *Technical mechanics*, 1, 5—19 [in Russian]. https://doi.org/10.15407/itm2020.01.005
11. Dolgopolov, S. I., Zavoloka, A. N., Nikolayev, O. D., Sviridenko, N. F., Smolensky, D. E. (2015). Determination of the parameters of hydrodynamic processes in the power system of the space stage during shutdowns and starts of the main engine. *Technical mechanics*, 2, 23—36 [in Russian].
12. Glikman, B. F. (1974). *Automatic control of liquid rocket engines*. Moscow: Mashinostroenie [in Russian].
13. Charny, I. A. (1961). *Unsteady motion of a real fluid in pipes*. Moscow: GITTL [in Russian].
14. Dolgopolov, S. I., Nikolayev, O. D. (2017). Mathematical modeling of low-frequency dynamics of the fluid flow controller at different amplitudes of harmonic disturbances. *Technical mechanics*, 1, 15—25 [in Russian].
15. Glikman, B. F. (1989). *Automatic control of liquid rocket engines*. Moscow: Mashinostroenie [in Russian].
16. Alemasov, V. E., Dregalin, A. F., Tishin, A. P. (1980). *Theory of rocket engines*. Moscow: Mashinostroenie [in Russian].
17. Natanzon, M. S. (1977). *Longitudinal self-oscillations of a liquid rocket*. Moscow: Mashinostroenie [in Russian].
18. Belyaev, E. N., Chervakov, V. V. (2009). *Mathematical modeling of LRE*. Moscow: MAI-PRINT [in Russian].
19. Oppenheim, B. W., Rubin, S. (1993). Advanced Pogo Stability Analysis for Liquid Rockets. *Journal of Spacecraft and Rockets*, 30(3), 360—383.
20. Pylypenko, O. V., Prokopchuk, A. A., Dolgopolov, S. I., Khoryak, N. V., Nikolayev, O. D., Pisarenko, V. Yu., Kovalenko, V. N. (2017). Mathematical modeling and stability analysis of low-frequency processes in the march LRE with generator gas afterburning. *Bulletin of engine building*, 2, 34—42 [in Russian].
21. Khoriak, N. V., Dolhopolov, S. I. (2017). Features of mathematical simulation of gas path dynamics in the problem of the stability of low-frequency processes in liquid-propellant rocket engines. *Technical mechanics*, 3, 30—44 [in Russian]. https://doi.org/10.15407/itm2017.03.030
22. Pylypenko, O. V., Khoriak, N. V., Dolhopolov, S. I., Nikolayev, O. D. (2019). Mathematical simulation of dynamic processes in hydraulic and gas paths at the start of a liquid-propellant rocket engine with generator gas after-burning. *Technical mechanics*, 4, 5—20. https://doi.org/10.15407/itm2019.04.005
23. Makhin, V. A., Prisnyakov, V. F., Belik, N. P. (1969). *Dynamics of liquid rocket engines*. Moscow: Mashinostroenie [in Russian].
24. Sobol, I. M., Statnikov, R. B. (1981). *Choice of optimal parameters in problems with many criteria*. Moscow: Nauka [in Russian].
25. Bendit, J., Pirsol, A. (1974). *Measurement and analysis of random processes*. Moscow: Mir [in Russian].

Received 22.03.2022
Revised 14.06.2022
Accepted 20.06.2022

О. В. Пилипенко (http://orcid.org/0000-0002-7583-4072),
С. І. Долгополов (http://orcid.org/0000-0002-0591-4106),
О. Д. Ніколаєв (http://orcid.org/0000-0003-0163-0891),
Н. В. Хоряк (http://orcid.org/0000-0002-4622-2376),
Ю. О. Кваша (http://orcid.org/0000-0002-5910-0407),
І. Д. Башлій (http://orcid.org/0000-0003-0594-9461)

Інститут технічної механіки Національної академії наук України
і Державного космічного агентства України,
вул. Лешко-Попеля, 15, Дніпро, 49005, Україна,
+380 56 372 0640, +380 56 372 0640, office.itm@nas.gov.ua

ВИЗНАЧЕННЯ РОЗКИДУ ТЯГИ БАГАТОДВИГУННОЇ УСТАНОВКИ І СТУПЕНЯ РАКЕТИ-НОСІЯ «ЦИКЛОН-4М» ПРИ ЇЇ ЗАПУСКУ

Вступ. Важливим напрямком роботи космічної галузі України є розробка космічного ракетного комплексу «Циклон-4М». Для зниження вартості, термінів розробки й виробництва рідинних ракетних двигунів (РРД) для І ступеня ракети-носія (РН) «Циклон-4М» ДП «КБ «Південне» використало в якості маршової двигунної установи І ступеня РН зв'язку декількох РРД, прототипи яких раніше були відпрацьовані.

Проблематика. У багатодвигунній установці запуск окремих двигунів за рахунок внутрішніх і зовнішніх факторів відбувається неодночасно. Це може призвести до небезпечних розкидів тяги окремих РРД в період запуску двигунної установки, які можуть викликати суттєві відхилення руху РН від її траєкторії на початковому етапі польоту.

Мета. Розрахункове визначення розкиду тяги при запуску багатодвигунної установки І ступеня РН «Циклон-4М», який обумовлено впливом внутрішніх і зовнішніх факторів на перехідні процеси в системах окремих двигунів та їх динамічною взаємодією.

Матеріали й методи. Використано методи теорії автоматичного регулювання, імпедансний метод, статистичний метод та методи чисельного моделювання неусталених процесів у трубопровідних системах РН.

Результати. Розроблено математичну модель запуску багатодвигунної установки І ступеня РН «Циклон-4М», яка дозволяє враховувати вплив розкидів внутрішніх і зовнішніх факторів на перехідні процеси в багатодвигунній установці при їх запуску. Розроблено ефективний метод визначення зазначеного розкиду тяги двигунів, який базується на використанні $ЛП_{\tau}$-рівномірно розподілених послідовностей. Визначено перехідні процеси в багатодвигунній установці РД-874 при різних поєднаннях розкидів зовнішніх і внутрішніх факторів, побудовано нижню та верхню огинаючі криві залежностей тиску в камері згоряння від часу для кожного РРД у складі багатодвигунної установки.

Висновки. Розкид часу набору 90 % тяги та набору тяги для багатодвигунної установки РД-874 в цілому є суттєво (приблизно в 2 рази) меншим, ніж для кожного двигуна РД-870 у складі цієї установки.

Ключові слова: рідинний ракетний двигун, багатодвигунна рідинна ракетна установка, запуск, математичне моделювання, зовнішні і внутрішні фактори, розкид тяги.